Self-assembly of stepped hollow oxide nanostructures with plasmonic–photonic properties

2008 J. Phys.: Condens. Matter 20 215217

(http://iopscience.iop.org/0953-8984/20/21/215217)

J. Phys.: Condens. Matter **20** (2008) 215217 (6pp) doi:10.1088/0953-8984/20/21/215217

Self-assembly of stepped hollow oxide nanostructures with plasmonic–photonic properties

Deeder Aurongzeb[1,3], **Latika Menon**[1] **and Bhargava K Ram**[2]

[1] Department of Physics, Northeastern University, Boston, MA 02115, USA
[2] Virginia Commonwealth University, Department of Electrical Engineering, Richmond, VA 23284, USA

E-mail: aurongzeb.d@neu.edu

Received 6 February 2008, in final form 12 March 2008
Published 22 April 2008
Online at stacks.iop.org/JPhysCM/20/215217

Abstract

We report the formation of hollow oxide nanostructures by oxidation of aluminum nanodots on gold thin film. The nanodots are formed by rapid thermal annealing of the thin film close to its melting point. The heights of the dots can be easily controlled via the initial thickness and temperature. The structure exhibits a phase transition when electrochemically oxidized and forms porous structure with a stepped interior. Despite the high level of disorder, a correlation length can be easily identified from the Fourier transformation of the surface. UV–visible spectroscopy and Fourier transform infrared spectroscopy show a stop gap at 1800 cm^{-1} showing the potential for photonic material application despite the high level of disorder.

(Some figures in this article are in colour only in the electronic version)

1. Introduction

Self-assembly on nanostructures has drawn a lot of attention recently due its potential for simple large-scale application [1–3]. During self-assembly processes interactions of different materials are the most dominant process. While a wide variety of interactions among the different phases of materials exist, oxidation and its effect on stress has always been a subject of intensive research among the scientific communities [4]. Generally, clean metal or semiconductor surfaces form passivating amorphous oxide film at or near room temperature whereas at high temperature thicker films form which are more crystalline in nature [5–8]. Lately, focus has mainly shifted toward nanoscale clusters as oxidized nanoscale clusters exhibit interesting physical and chemical properties. For example, Aumann *et al* [9] found that increasing surface area lowers the oxidation activation energy. Also, Zhou *et al* [10] recently showed how terraced hollow oxide can be formed due to high temperature oxidation of Cu. More recently, Omi *et al* showed that oxidation of silicon can lead to a phase transition in the universality class [11]. In all these previous studies, high temperature fast thermal oxidation was the main focus.

Recently, chemical oxidation, especially electrochemical oxidation of aluminum, has drawn a lot of attention due to its potential to create useful nanostructures [12, 13]. In this process, using appropriate current and voltage very ordered porous structure can be created by electrochemical oxidation. In all of the previous studies, films or foils with wide ranges of thicknesses were studied with the goal of obtaining and understanding ordered porous structures.

In this paper, we study structure formation due to oxidation of nanodots. We show a phase transition in the universality class during oxidation by forming cavities with 'devil's staircase' [14] type interiors. Historically, 'devil's staircase' refers to a path between Kingshouse and Kinlochleven in Scotland with a huge number of discrete steps. In condensed matter physics, the term indicates long-range elastic interaction that results in the formation of facets. We also show that the structures are fractal dielectric with photonic properties. The structures can reduce reflectance by more than 90% in a wide range of UV–IR spectra. We choose aluminum, as fundamental elastic information concerning aluminum and its oxide is readily available. Oxidation of well-separated nanodots is interesting because they form different sizes and shapes on different substrates [15, 16]. Therefore, wide ranges

[3] Author to whom any correspondence should be addressed.

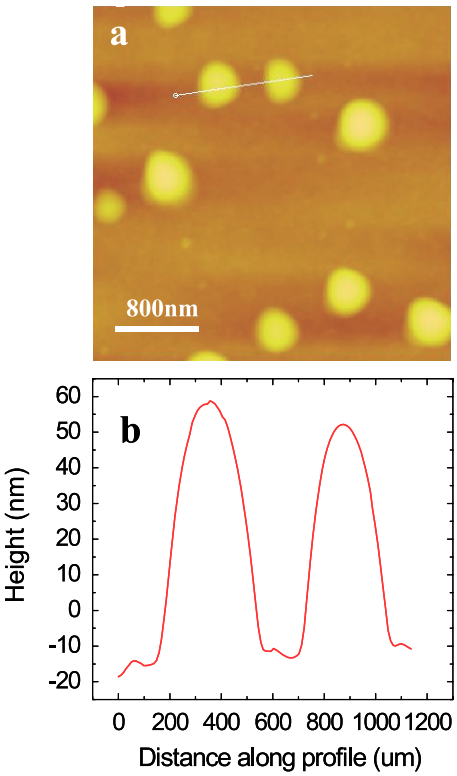

Figure 1. (a) Formation of nanodots from 50 nm thick aluminum films after rapid thermal annealing at 600 °C. (b) Line profile of the nanodots showing a dome shaped structure.

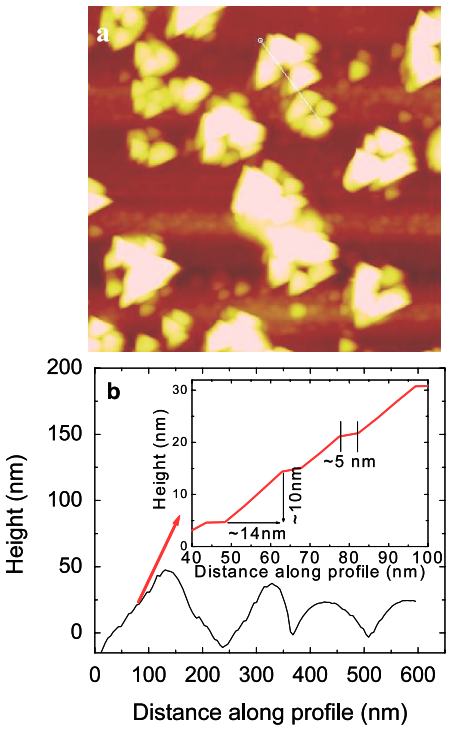

Figure 2. (a) Pore structure formation with 50 nm aluminum with step structure shown in the inset. (b) Line profile of the pore structure.

of structures can be obtained using appropriate materials and substrates.

2. Experimental details

The structure is mainly fabricated in two steps; self-assembly of aluminum nanodots from thin film by rapid thermal annealing and anodization of nanodots to form staircase-like structure. About 10 nm of gold was thermally deposited on glass wafers followed by 50, 70 and 100 nm of aluminum thin film. The samples were then annealed in a fast thermal anneal chamber to form the nanodots. The purpose of the gold layer is simple: to provide conduction paths between the power supply and the nanodots. Any conducting material can be used as long as the melting point of the material is higher than the melting point of nanodot forming material. This is simply to avoid any interdiffusion and open circuits during anodization. We found that 50 nm is the lowest thickness where the nanodots are organized and big enough to form semi-organized structure. Detail of the deposition conditions can be found in [17]. The samples were annealed at 600 °C for ∼10 min. This temperature is very close to the melting point of aluminum (∼660 °C); hence very fast diffusion within aluminum is attainable while gold is reasonably stable. It is possible to have some interdiffusion take place while the dots are forming but the process does not effect the formation of nanodots. The process results in formation of aluminum nanodots as shown in figure 1(a). The nanodots are ∼60 nm in height and ∼400 nm in diameter. This information was very important because we found that dot height imitates initial film thickness. Therefore, height and width of the structures can be controlled using proper thickness and temperature. The samples were then anodized in 3% oxalic acid with 50 V, 0.1 A current for ∼5 min. This process resulted in formation of alumina nanostructure with staircase-like interior. We have verified that dot formation and alumina nanocrystal formation can be controlled up to 100 nm aluminum thickness (figure 4). Optical properties were verified with a UV–visible spectrometer and Fourier transform infrared spectrometer (FTIR). To identify typical surface processes for these structures, we calculate the height–height correlation function (HCF). HCF is defined as

$$\mathrm{HCF}(r,t) = \sqrt{\langle |h(r-r') - h(r')|^2 \rangle} \qquad (1)$$

where $h(r')$ is the surface height at position r' $(=(x, y))$ on the surface relative to the average surface height. For arbitrary surfaces, HCF scales as HCF $\sim r^{\alpha}$ and the fractal dimension is given by [18]

$$D = d - \alpha \qquad (2)$$

where d is the dimension. In this case, the method uses a height–height correlation function of dimension 2. The advantage of this method is that without knowing detail of the interaction we can have better understanding of interface growth processes based on internal symmetries and dimension.

3. Results and discussion

Figure 2(a) shows formation of alumina with stepped interior. The dots were about 60 nm in height; therefore, the height of

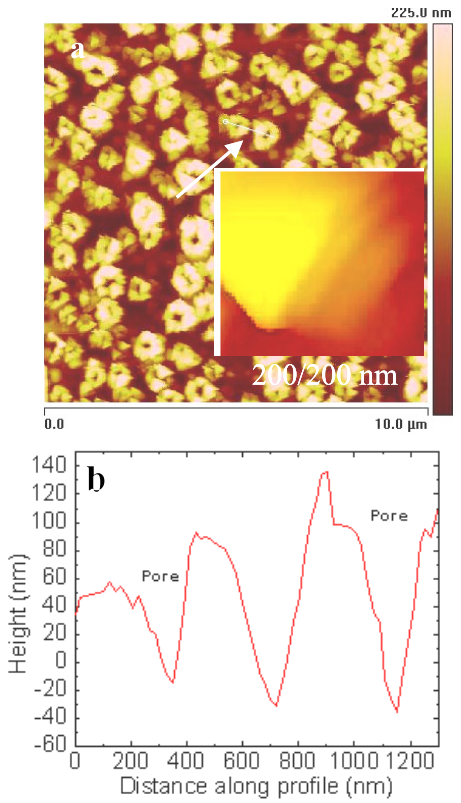

Figure 3. (a) Pore structure formed from 100 nm dots. (b) Line profile of the pore structure with AFM of stepped structure (inset).

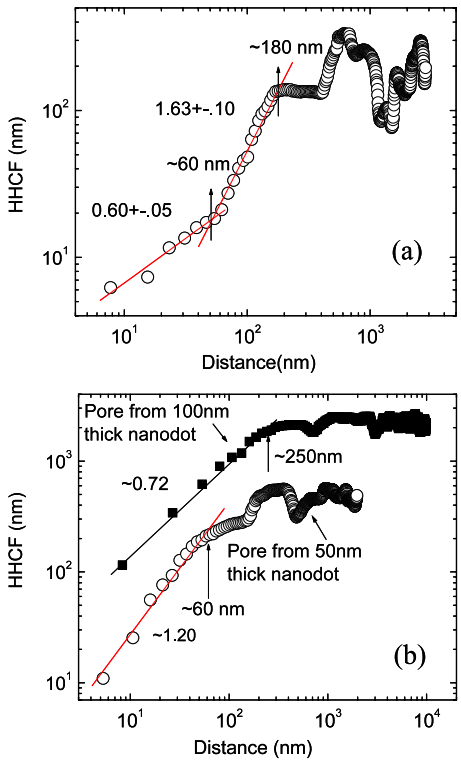

Figure 4. (a) Height–height correlation function for nanodots made with 50 nm thick aluminum. (b) Height–height function for anodized structure; 50 nm (bottom) and 100 nm (top).

the oxide structure is expected to imitate the nanodot height. Figure 2(b) shows typical pore depth, which is similar to overall film thickness as expected. The pore interior is clearly staircase type. Later, we will show that the steps are non-monotonic and faceted, hence showing characteristics of a 'devil's staircase' [14]. The inset of figure 2(b) shows typical dimensions of the steps. Since nanodots are self-assembled by annealing the thin films and by manipulating the fact that aluminum has very low melting point, some interdiffusion is possible and dot size can vary resulting in an erratic pore structure. However, for 100 nm thick aluminum film, nanodots are well formed and separated and when anodized, the pores are well formed and dense. Figure 3(b) shows an alumina structure formed with well-structured interior from bigger nanodots (100 nm). The formation of these structures is very similar to that of other oxide systems. For example, when copper films are oxidized, instead of forming uniform layers they tend to grow as oxide islands and they can be self-limiting after certain thicknesses [19]. For our case, we can assume similar situations, where the primary reason for formation of the structures is stress inside the oxide. For compressive stress it is required that the volume of metal ions in the oxide is bigger than the volume of metal in the metal. For most metal this is true and for aluminum the value is 1.28 [1]. Therefore, for this case the stress is compressive. Generally for thin film systems, oxide forms through random nucleation sites. For electrochemical oxidation the sites are preferential. For example, tips of the nanodots have higher electric field and will oxidize faster than the sidewalls. Therefore, stress will build up faster at the top than on the sidewalls. Since the nanodots have triangular/conic profiles (figure 1, line profile) less force will be required to cause plastic slip at the top. Hence, due to fast build up of high stress, the nanodot tips will have bigger openings than the bottom and thus should have tilted pore walls. This is clearly seen in the figures 2(b) and 3(b) where the pore inner wall is slanted and stepped with a step height of ∼10 nm. The observed step height is also consistent with previous observations made for planar film [20, 21]. It has been shown that for lattice mismatch f, where f is given by

$$f = [2a(\mathrm{Al})/a(\mathrm{oxide})] - 1 \qquad (3)$$

where a is the unstrained lattice constant, the critical thinness when plastic deformation is important is ∼4 nm. The variation in the step height for nanodots could be due to several factors including compression due to sidewall oxidation and fluctuation of local electric field.

Figure 4 shows the roughness exponent calculation based height–height correlation function. Figure 4(a) shows two exponents for nanodots, formed with 50 nm thick aluminum thin film and figure 4(b) shows exponent values after anodization including the thicker (100 nm) case. As seen in figure 4(a), the global roughness exponent is >1.5. The value of $\alpha > 1$ generally suggests that the surface is super-rough [22]. In this case the local surface width does not saturate and crosses over to a different behavior. Surface processes exhibiting such behavior are generally called anomalously scaling [23]. Although there is no well-understood theory of anomalous scaling, it has been suggested

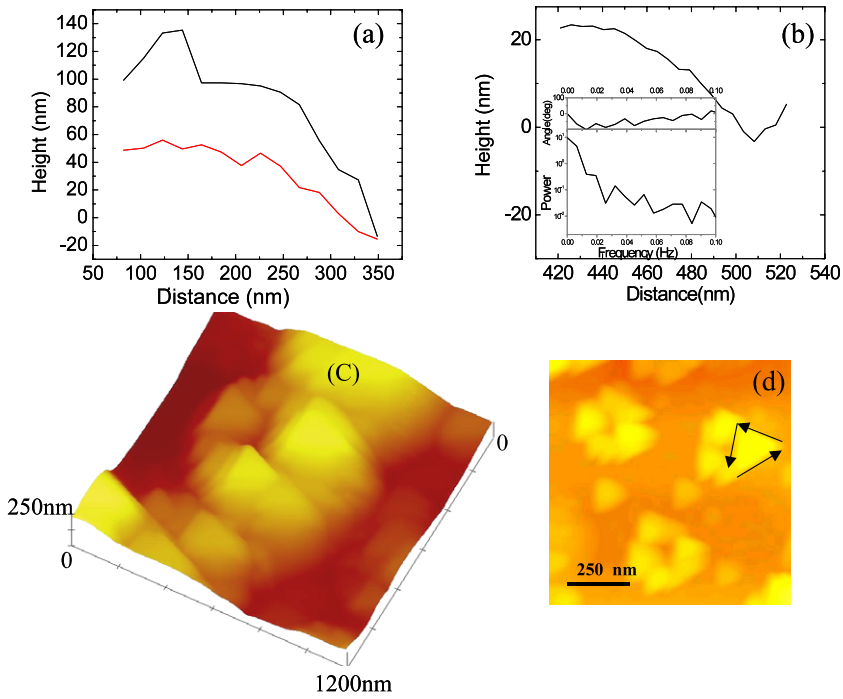

Figure 5. (a) Representative line profile of steps for large structures. (b) Line profile of a smaller structure with FFT of the profile showing non-monotonic nature of the profile. (c) 3D AFM image of a single structure clearly showing the steps and cavity. (d) Early stage of formation using thin (∼30 nm) layers of aluminum showing triangular structure, as a primary building block for the steps.

that it must be due to non-local effects [24]. Aluminum nanodots formed by annealing close to the melting point have several such effects. An important one is rapid jumping in the interface position. Observe that nanodots are well separated, with 60 nm height consistent with this case. Therefore, with more dense and rough structure the anomalous scaling should vanish. We find that this is indeed the case. After anodization we find that the system lacks anomalous scaling and the roughness exponent drops even further for denser anodized nanodots as seen in figure 4(b). The detail of surface processes for nonlinear and linear cases described by Das Sarma *et al* [25] using Monte Carlo simulations in 2D follows. For the linear case, it is found that only isolated atoms can diffuse and will stick to the nearest kink site. Therefore, movement of clusters should be minimal during oxidation and as they touch other oxidized sites they become pinned and aggregate until the compressive stress is high enough to cause slip. For small nanodots (50 nm), this is not immediately visible due to large and sudden interface fluctuation. For more dense and ordered structure at 100 nm structure level, this is clearly seen.

Cluster formation and aggregation can be easily determined from the fractal dimension. We find that the fractal dimension is ∼1.3 in 2D for figure 3(a) as calculated from figure 4(b). The fractal dimension agrees well with the cluster–cluster aggregation model [26]. We should mention here that the model only provides a general description of the process, not addressing the intricate detail. In particular, formations with tilts, different facets and disorder evolving are not taken into account.

Figures 5(a) and (b) show some representative step profiles for various size dots. Clearly seen steps are not correlated and have various facet angles. Fast Fourier transformation (figure 5(b), inset) of the profile figure 5(b) shows that the steps are non-monotonic; therefore they are 'devil's staircase' type. Figure 5(c) clearly shows steps with well-defined cavities. To understand the elementary building block of these structures we performed an experiment with low thickness (∼30 nm) nanodots and found that the steps are made of triangular blocks as shown in figure 5(d). This observation is different to previous observations of structures found for high temperature oxidation. Formation of a 'devil's staircase' also suggests that a competing mechanism is present in the system that led to the formation of these structures.

Figure 6 shows reflectivity measurements at various steps of the alumina formation process. We find a drop in reflectivity by 90% in UV–visible range. We find that the reduction is over a broad range of the spectrum, with absorption. We believe one of the main reasons is the location of Au thin film beneath the pore structure. Figure 6 shows that Au itself can reduce reflectivity over broad range of wavelengths, by absorption of 40%. This is consistent with the fact that oxide nanostructure covers about 70% of the surface. Coupling between these structures can result in an observed broadening. While our resources limit us, other conducting material or conducting oxide can eliminate this problem. Figure 7 shows the FTIR spectrum of the structure. The FTIR spectrum for glass substrate is also shown for comparison. The structure clearly suppresses reflectance for the glass peaks with ∼95% reflectance at 1300 cm^{-1} (7.5 μm). We believe that the high reflectance in the IR is cavity resonant type. The first signature is the asymmetric nature of the transmission, indicating cavity resonance and Fabry–Perot oscillation coupled. The second

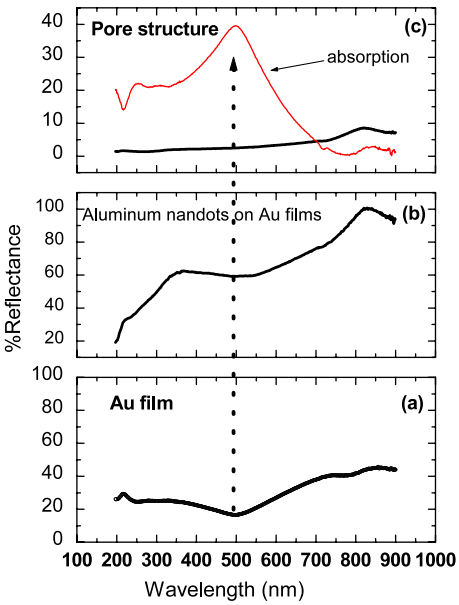

Figure 6. UV–visible reflectivity measurements for structures formed at different stages. (a) Reflectivity of Au film on glass. Observe the depth in the spectral scan at ∼500 nm. (b) Reflectivity measurement of aluminum nanodots on gold film. (c) Reflectivity of the final system. Also shown (in red): absorption measurement of the final structure. Observe the depth observed at 500 nm for Au film coinciding with the absorption of the Au/hollow oxide system at that wavelength as shown by the arrow. Clearly seen is the absorption and broadening being due to Au (dotted arrow). For the final system: 90% drop in reflectivity measured at 45° in the UV–visible range.

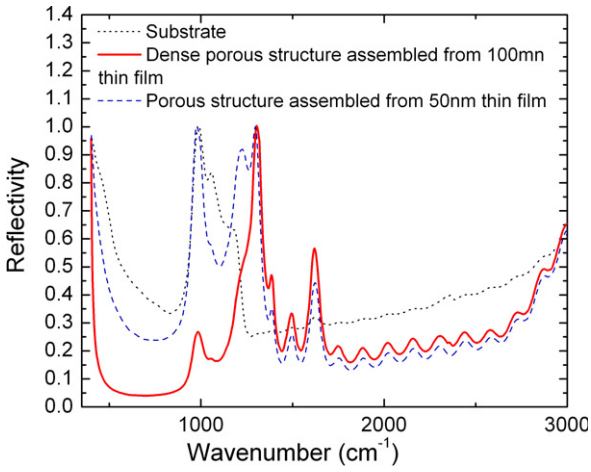

Figure 7. Fourier transformed infrared spectrum of pore structures with different thicknesses. >95% reflection at ∼7.5 μm.

indication came from experimental reflectivity as shown for less dense cases (50 nm film). Clearly seen is the cavities being more dispersed as the reflectivity is more coupled to the background, which in this case is glass.

4. Conclusion

In conclusion, we show the formation of large nanodots by driving the interface close to its melting point. Using this for nanodots we have shown a simple method for self-assembling dielectric nanocrystal with slanted pore 'staircase'-like interior. The reflectivity results suggest that complex-coupling phenomena exist, between the cavities, and these structures can act as a photonic material. In the light of recent development in complex photonic structures [27, 28] we believe very complex dielectric structures can be made using metal that forms different crystalline facets. We have left out two effects in this work. One is Au/Al interaction in terms of nanodot formation and island–island interaction for size distribution. Since the heat of melting [29] for Au (17.8 kJ mol^{-1}) is 1.5 times that for Al for a short anneal, we do not expect enough interaction to affect the nanodot formation. While the effect of surface energy and substrate–film stress interaction on the density of nanodots can be similar to that for other low temperature annealed nanodot systems, melting point driven bimetallic systems require more rigorous schemes. Detail of that study will be published somewhere else.

Acknowledgment

This work was partially supported by NSF grants nos ECS-0348156 and ECS-0304224.

References

[1] Lee W, Nielsch K and Gösele U 2007 *Nanotechnology* **18** 475713
[2] Rahedi A J, Douglas J F and Starr F W 2008 *J. Chem. Phys.* **128** 024902
[3] Keenan C, Chandril S, Myers T H, Lederman D, Ramos-Moore E and Cabrera A L 2008 *Appl. Phys. Lett.* **92** 013119
[4] Hancock P and Hurst R C 1974 *Advances in Corrosion Science and Technology* ed R W Staehle and M G Fontana (New York: Plenum)
[5] Doherty P E and Davis R S 1963 *J. Appl. Phys.* **34** 619
[6] Reversz A G and Fehlner F P 1981 *Oxid. Met.* **15** 297
[7] Fehlner F P 1981 *Low-Temperature Oxidation: the Role of Vitreous Oxides* (New York: Wiley-Interscience)
[8] Lawless K R 1973 *Rep. Prog. Phys.* **37** 231
[9] Aumann C E, Skofronick G L and Martin J A 1995 *J. Vac. Sci. Technol.* B **13** 1178
[10] Zhou G, Slaughter W S and Yang J C 2005 *Phys. Rev. Lett.* **94** 246101
[11] Omi H, Kageshima H and Uematsu M 2006 *Phys. Rev. Lett.* **97** 016102
[12] Masuda H and Fukuda K 1995 *Science* **268** 1466
[13] Watanabe K, Takemura Y, Shimazu Y and Shirakashi J 2004 *Nanotechnology* **15** S566
[14] Ackland G J 2002 *Phys. Rev.* E **66** 041605
Krack B D, Ozoli V, Asta M and Daruka I 2002 *Phys. Rev. Lett.* **88** 186101
Bak P and Bruinsma R 1982 *Phys. Rev. Lett.* **49** 249–51
Mandelbrot B 1977 *Fractals: Form, Chance, and Dimension* (San Francisco, CA: Freeman)
[15] Aurongzeb D, Washington E, Basavaraj M, Berg J M, Temkin H and Holtz M 2006 *J. Appl. Phys.* **100** 114320
[16] Aurongzeb D, Bhargava Ram K, Holtz M, Basavaraj M, Kipshidze G, Yavich B, Nikishin S A and Temkin H 2006 *J. Appl. Phys.* **99** 014308
[17] Aurongzeb D 2005 *Appl. Surf. Sci.* **252** 872
[18] Goluvobic L and Bruinsma R 1991 *Phys. Rev. Lett.* **60** 321

[19] Yang J C, Kolasa B, Gibson J and Yeadon M 1998 *Appl. Phys. Lett.* **73** 2841
[20] Jeurgens L P H, Sloof W G, Tichelaar F D and Mittemeijer E J 2000 *Phys. Rev.* B **62** 4707
[21] Doherty P E and Davis R S 1963 *J. Appl. Phys.* **34** 619
[22] Das Sarma S, Ghaisas S V and Kim J M 1994 *Phys. Rev.* E **49** 122
[23] López M, Rodríguez M A and Cuerno R 1997 *Physica* A **246** 329
[24] López J M, Castro M and Gallego R 2005 *Phys. Rev. Lett.* **94** 166103
[25] Das Sarma S and Ghaisas S V 1992 *Phys. Rev. Lett.* **69** 3762
Das Sarma S and Ghaisas S V 1993 *Phys. Rev. Lett.* **71** 2510
[26] Meakin P 1983 *Phys. Rev. Lett.* **51** 1119
[27] Junji Tominaga M H 2003 *J. Phys.: Condens. Matter* **15** R1101
[28] Nair R V and Vijaya R 2007 *J. Phys. D: Appl. Phys.* **40** 990
[29] Lee B-J, Shim J-H and Baskes M I 2003 *Phys. Rev.* B **68** 144112